Brief Communications

An Early Critical Period for Long-Term Plasticity and Structural Modification of Sensory Synapses in Olfactory Cortex

Cindy Poo and Jeffry S. Isaacson
Department of Neuroscience, University of California, San Diego, School of Medicine, La Jolla, California 92093

Critical periods for plasticity of thalamic sensory inputs play an important role in developing neocortical circuits. During an early postnatal time window, pyramidal cells of visual, auditory, and somatosensory cortex undergo structural refinement and possess an enhanced ability for activity-dependent synaptic plasticity. In olfactory cortex, however, pyramidal cells receive direct sensory input from the olfactory bulb, and it is unclear whether the development of olfactory sensory circuits is governed by a critical period. Here, we show that NMDA receptor-dependent long-term potentiation and dendritic spine maturation occur only during a brief postnatal time window at sensory synapses of olfactory cortex pyramidal cells. In contrast, associational synapses onto the same cells retain the capacity for plasticity into adulthood.

Key words: **piriform cortex; LTP; spines; LOT; olfaction; development**

Introduction

In the visual, auditory, and somatosensory systems, sensory experience modifies cortical circuits during a short, postnatal "critical period" after which synaptic reorganization is difficult to induce (Katz and Shatz, 1996; Hensch, 2004). However, little is known about the mechanisms governing the early development and plasticity of olfactory circuits.

Olfactory sensory information is conveyed from olfactory receptor neurons (ORNs) in the nasal epithelium to the olfactory bulb. Here, ORNs expressing unique types of odorant receptors project to stereotyped subsets of principal mitral cells, which are thought to represent a spatial map of odor information (Ressler et al., 1994; Mombaerts, 2001). However, the coding of odor quality and olfactory perception itself ultimately involves the activity of neurons in higher brain regions.

Primary olfactory (piriform) cortex is a major cortical region believed to play an important role in the representation of olfactory information (Haberly, 1998). Axons of olfactory bulb mitral cells coalesce in the lateral olfactory tract (LOT) and make dense connections with pyramidal cells of the anterior piriform cortex. This afferent sensory input targets the distal apical dendrites of layer II/III pyramidal cells (Price, 1973), whereas associational (ASSN) fibers from various cortical regions target proximal apical and basal dendrites (Haberly and Presto, 1986; ul Quraish et al., 2004). Given the precise mapping of particular odor features onto mitral cells, it may be that LOT sensory synapses in olfactory cortex are "hardwired" for the coding of olfactory information. For example, to maintain an invariant representation of specific odor features, activity-dependent plasticity of LOT inputs may not necessarily be desirable. Consistent with this notion, previous studies of LOT-evoked field EPSPs (fEPSPs) in adult rat olfactory cortex slices found that NMDA receptor (NMDAR)-mediated long-term potentiation (LTP) was not reliably induced by tetanic stimulation (Jung et al., 1990). Successful LTP induction was difficult to achieve and resulted in only modest (10–15%) increases in synaptic strength (Jung et al., 1990; Kanter and Haberly, 1990; Kanter and Haberly, 1993). However, given that NMDARs contribute more to LOT transmission in neonatal cortex (Franks and Isaacson, 2005), sensory synapses in piriform cortex may have an enhanced capacity for plasticity during early postnatal development.

Newborn animals (including humans) use olfactory information to form strong maternal attachments, and this "imprinting" to maternal odors is crucial for survival in many species (Leon, 1992; Sullivan, 2003). This strong behavioral plasticity is limited to neonatal animals. These findings imply that in addition to being both functional and necessary at birth, central olfactory circuits could display enhanced plasticity during the early postnatal stage. However, it is unknown if the plasticity and maturation of synaptic transmission in the olfactory cortex could underlie this developmental time window for imprinting.

In this study, we examine whether a critical period for synaptic plasticity and structural development may occur in olfactory cortex. We use whole-cell recording to investigate NMDAR-dependent LTP at sensory LOT inputs and ASSN synapses onto the same pyramidal cells. We find that LOT inputs express robust LTP in neonatal animals; however, the magnitude of LTP at these

Received Feb. 12, 2007; revised June 7, 2007; accepted June 9, 2007.

This work was supported by National Institute on Deafness and Other Communication Disorders Grant R01DC04682.

Correspondence should be addressed to Dr. Jeffry S. Isaacson, Department of Neuroscience, MC 0634, Center for Molecular Genetics, Room 213, University of California, San Diego, School of Medicine, 9500 Gilman Drive, La Jolla, CA 92093-0634. E-mail: jisaacson@ucsd.edu.

DOI:10.1523/JNEUROSCI.1786-07.2007

 0270-6474/07/277553-06$15.00/0

sensory synapse declines rapidly during the first month of postnatal development. In contrast, the capacity of ASSN inputs to express robust NMDAR-dependent LTP remains throughout adulthood. In addition, we also characterize the maturation of dendritic spines in pyramidal cell dendritic regions primarily devoted to LOT or ASSN synapses. We find a more rapid maturation of dendritic spines at the site of LOT input compared with ASSN synapses. Together, these results suggest a developmental critical period for the plasticity of olfactory sensory inputs in piriform cortex.

Materials and Methods

Electrophysiology. Piriform cortex slices (~400 μm) were prepared from postnatal day 5 (P5) to P35 Sprague Dawley rats in accordance with institutional and national guidelines using standard procedures. Parasagittal cortical slices were cut using a vibrating slicer (Vibratome, St. Louis, MO) in ice-cold artificial CSF (aCSF) containing (in mM) 83 NaCl, 2.5 KCl, 0.5 $CaCl_2$, 3.3 $MgSO_4$, 1 NaH_2PO_4, 26.2 $NaHCO_3$, 22 glucose, and 72 sucrose, equilibrated with 95% O_2/5% CO_2 at 34°C for 30 min and at room temperature thereafter. In the recording chamber, slices were viewed by means of infrared-differential interference contrast (IR-DIC) optics (BX-51W1; Olympus, Tokyo, Japan) and superfused with aCSF containing (in mM) 119 NaCl, 5 KCl, 4 $CaCl_2$, 4 $MgSO_4$, 1 NaH_2PO_4, 26.2 $NaHCO_3$, 22 glucose, and 0.1 picrotoxin, equilibrated with 95% O_2/5% CO_2. The high divalent concentrations (4 mM Ca^{2+} and 4 mM Mg^{2+}) were used to suppress spontaneous epileptiform activity in the presence of the $GABA_A$ receptor antagonist picrotoxin. All experiments were performed at 30–32°C. Baclofen (30 μM) was added to the aCSF to suppress ASSN inputs when isolated LOT inputs were examined (Franks and Isaacson, 2005).

Patch electrodes (3–5 MΩ) contained (in mM) 130 D-gluconic acid, 130 CsOH, 5 NaCl, 10 HEPES, 12 phosphocreatine, 3 MgATP, 0.2 NaGTP, and 0.2 EGTA. Series resistance, which was <15 MΩ, was compensated at 80–95%. The uncorrected liquid junction potential in these recordings was ~12 mV. Synaptic currents were recorded with an Axopatch 200B amplifier (Molecular Devices, Foster City, CA), filtered at 2–5 kHz, collected, and digitized at 10–20 kHz (ITC-18; InstruTech, Mineola, NY). Data acquisition and analysis were performed with Axograph 4.9 (Molecular Devices) and IGOR Pro 4 (Wavemetrics, Lake Oswego, OR) software.

Pyramidal cells for all experiments had cell bodies in deep layer II. Sensory and ASSN EPSCs were evoked using focal stimulating electrodes (1 MΩ pipettes filled with aCSF) placed in the LOT or layer II/III, respectively. Stimulating electrodes were positioned ~150 μm laterally from the recorded cell. The amplitudes of EPSCs were measured over a 0.5–1 ms window centered at the peak of the response. Stimulus strength was set such that EPSCs were 100–200 pA in amplitude under baseline conditions. For the "pairing" protocol, a 5 min baseline was monitored (V_m = −80 mV) using 0.2 Hz stimulation. The cell was then depolarized to 0 mV, and 40 paired-pulse stimuli [50 ms interstimulus interval (ISI)] were delivered at 0.2 Hz. The membrane potential of the cell was then returned to −80 mV after the pairing procedure, and 0.2 Hz stimulation was continued to monitor EPSC amplitude. Pairing was always performed within 5–7 min of breaking into a cell. The magnitude of LTP was determined from the average amplitude of EPSCs 25–30 min after pairing. Summary results and figures include every experiment in which pairing was performed after a stable baseline response was recorded for 5 min. All results represent mean ± SEM.

Imaging. For experiments examining dendritic spines, Alexa 488 (50 μm) was added to the patch electrode internal solution. Imaging was performed with an Olympus Fluoview 300 system modified for two-photon laser microscopy using a femtosecond laser (MaiTai; Spectra-Physics, Mountain View, CA) tuned to 800–820 nm. Distal apical dendrite segments were used to quantify spines receiving sensory input. All distal apical dendritic regions were verified under IR-DIC optics to overlap with LOT fibers. We restricted measurements of ASSN spines to regions of basal dendrite and proximal apical dendrite (within ~50–100 μm of the soma depending on age). Image stacks (600× magnification, 512 × 512 pixels, 10–20 frames with 0.5 μm steps) were taken of distal apical dendrites and secondary or tertiary proximal apical and basal dendrites. Image stacks were collapsed onto a *z*-projection using maximal intensities from each frame. All image and data analyses were performed with ImageJ (National Institutes of Health, Bethesda, MD) and IGOR Pro 4 (Wavemetrics) software. Dendritic protrusion densities and lengths were averaged across all dendritic segment images obtained from each cell. On average, two to five dendritic segments from each dendritic compartment were pooled for each cell. All analyses were performed blind to the age of animals and to the dendritic compartments of cells.

Results

Previous reports of activity-dependent plasticity at sensory synapses in olfactory cortex monitored the effect of theta-burst or tetanic stimulation on LOT-evoked extracellular fEPSPs (Jung et al., 1990; Kanter and Haberly, 1990, 1993; Stripling et al., 1991). We used whole-cell recording to study LOT-evoked EPSCs recorded from layer II pyramidal cells in rat anterior piriform cortex slices (Franks and Isaacson, 2005). In newborn rats (P5–P10), we alternately stimulated two independent LOT inputs (each input at 0.2 Hz) onto a single voltage-clamped pyramidal cell (V_m = −80 mV) (Fig. 1A_1). Glass focal stimulating electrodes were positioned in the LOT and bracketed the recorded pyramidal cell with a spacing of ~100 μm. The independence of the two LOT pathways was always confirmed by verifying that simultaneous stimulation of the two pathways produced an EPSC in the pyramidal cell that was the algebraic sum of the EPSCs produced by stimulation of each pathway alone.

To investigate NMDAR-dependent LTP, we used a pairing protocol (see Materials and Methods), the goal of which is to "pair" presynaptic stimulation with postsynaptic depolarization. After a baseline period of 5 min, the neuron was depolarized to 0 mV to remove the voltage-dependent Mg^{2+} block of NMDARs. During this depolarization, only one of the two pathways (the "paired" pathway) was stimulated. The other pathway ("unpaired") thus served as control for the depolarization alone. This produced an LTP of EPSCs (78 ± 11%; n = 9; range, 46–134%) in the paired pathway, whereas the EPSCs of the unpaired pathway were unaffected (Fig. 1A_2). This pairing-induced LTP demonstrates that synapse specific plasticity at sensory LOT synapses does not require widespread activation of fibers through tetanic stimulation.

Previous studies of LOT-evoked field potentials demonstrated that LTP induced by theta-burst stimulation is blocked by the NMDAR antagonist APV (Jung et al., 1990; Kanter and Haberly, 1990). To confirm the role of NMDARs in pairing-induced LOT LTP, in a subsequent set of experiments, we interleaved pairing of a single pathway in control slices (80 ± 3%; n = 5; range, 30–126%) with slices maintained in the presence of APV (100 μM; n = 5). In the presence of APV, pairing-induced LTP was abolished (Fig. 1A_3) (Student's t test, $p < 0.05$). In a subset of experiments (Fig. 1A_2,A_3), we used paired-pulse stimulation (50 ms, ISI) to monitor presynaptic function during LTP. LOT synapses showed paired-pulse facilitation (EPSC2/EPSC1), which was unchanged during LTP (Fig. 1A_4) (paired Student's t test, $p = 0.90$), consistent with a postsynaptic locus for LTP expression (Nicoll and Malenka, 1999). Together, these results show that synapse-specific, NMDAR-dependent LTP can be triggered at olfactory sensory inputs of newborn rats.

In contrast to neonatal rats, we found that plasticity of sensory synapses was markedly reduced in animals that were slightly older (P15–P19). In these experiments, we monitored the strength of LOT and ASSN inputs onto the same pyramidal cells

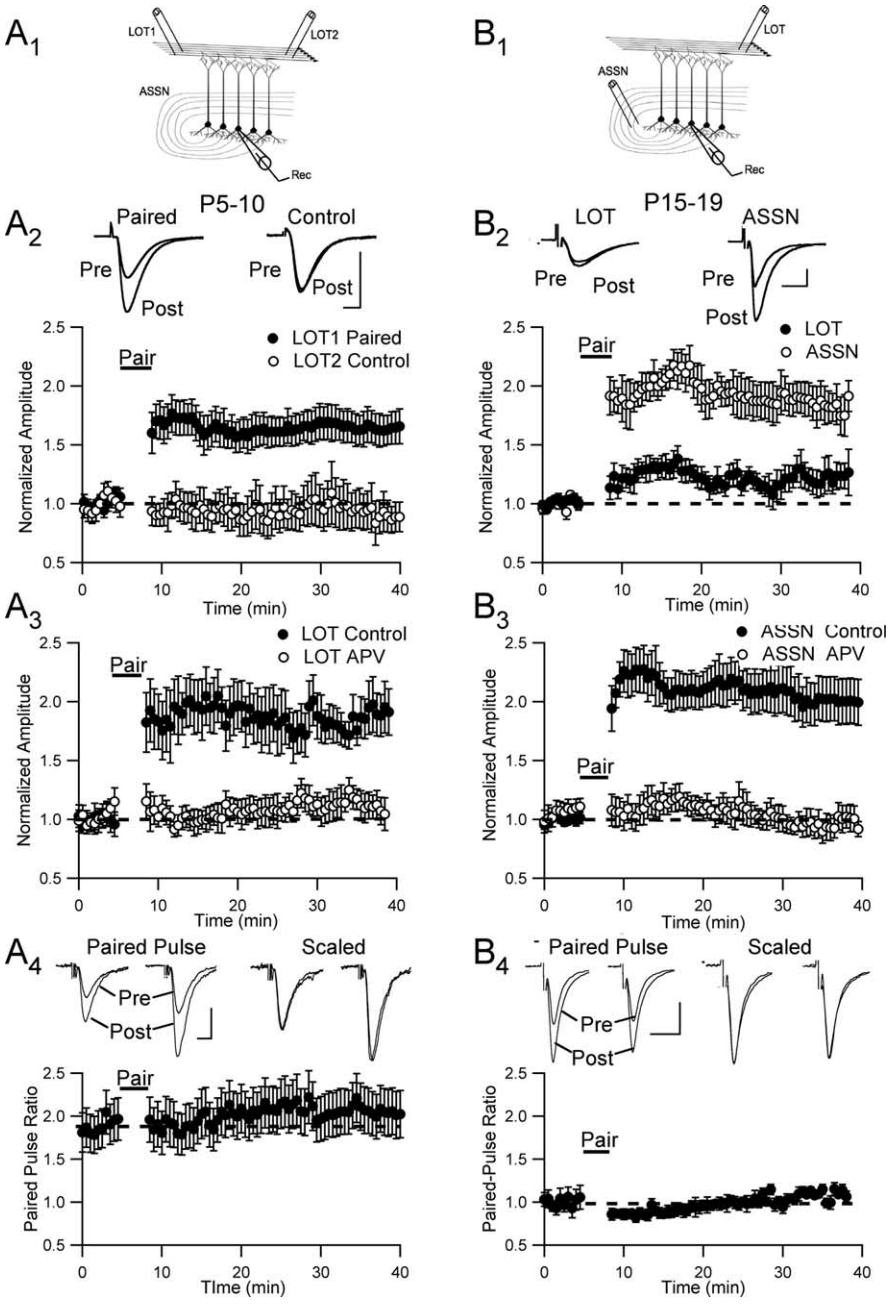

Figure 1. NMDAR-dependent LTP of sensory and ASSN synapses in olfactory cortex. ***A***, Synaptic plasticity of LOT synapses in P5–P10 rats. ***A*$_1$**, Recording configuration. ***A*$_2$**, Pairing stimulation of one LOT pathway with depolarization induces LTP (filled circles), whereas the unpaired pathway (open circles) is unaffected. Traces show EPSCs from one cell before and 30 min after LTP induction at paired (left) and control (right) inputs. ***A*$_3$**, APV prevents the induction of LTP at LOT synapses (open circles), whereas interleaved control recordings (filled circles) show robust LTP. ***A*$_4$**, LTP of LOT synapses in ***A*$_2$** and ***A*$_3$** does not alter the paired-pulse ratio ($n = 11$). Traces before and 30 min after LTP induction from one cell are superimposed (left) and scaled (right). ***B***, Synaptic plasticity of LOT and ASSN synapses in P15–P19 rats. ***B*$_1$**, Recording configuration. ***B*$_2$**, Pairing both LOT and ASSN inputs elicits robust LTP at ASSN synapses (open circles) and weak LTP at LOT synapses (filled circles). ***B*$_3$**, APV blocks LTP induction at ASSN synapses. ***B*$_4$**, LTP of ASSN synapses in ***B*$_2$** is not accompanied by a persistent change in the paired-pulse ratio ($n = 5$). Calibration: 5 ms, 100 pA. Rec, Recording; Pre, before; Post, after.

(Fig. 1B_1) and paired stimulation with membrane depolarization in both pathways. Compared with the P5–P10 age group, the amount of LTP induced at LOT synapses was drastically reduced (26 ± 11%; $n = 7$; range, 9–62%). In these same cells, ASSN synapses potentiated strongly (91 ± 13%; $n = 7$; range, 72–188%) (Fig. 1B_2) ($n = 7$). Increasing the number of EPSCs paired with depolarization did not lead to greater LTP at LOT synapses (data not shown), indicating that our pairing procedure yielded the maximal amount of potentiation. Interleaving control slices with those in the presence of APV ($n = 5$ and 8, respectively) revealed that LTP of ASSN synapses required activation of NMDARs (Fig. 1B_3) (Student's t test, $p < 0.05$). Under our conditions, ASSN synapses show weak paired-pulse depression at an ISI of 50 ms, and there was no change in the ASSN paired-pulse ratio after induction of LTP (Fig. 1B_4) (paired Student's t test, $p = 0.79$). Thus, like LOT inputs, ASSN synapses also exhibit pairing-induced postsynaptic expression of NMDAR-dependent LTP.

We recorded from olfactory pyramidal cells throughout the first month of postnatal life and found a significant decrease in the amount of LTP expressed at sensory synapses by the second postnatal week (Fig. 2). A consistent decrease in the amount of LTP expressed at LOT synapses was observed at later developmental time points. By the fourth postnatal week, LOT synapses failed to express any long-term plasticity. In sharp contrast, robust LTP could be elicited at ASSN synapses of the same pyramidal cells throughout this developmental time window, with no obvious difference in the magnitude of potentiation at any time point. We performed regression analysis on the two data groups to determine the differences in correlation of LTP amplitude versus age. For LOT synapses, a linear regression yielded $R^2 = 0.92$, with a correlation coefficient p value of 0.0091, whereas for ASSN synapses, $R^2 = 0.19$ and the correlation coefficient p value is 0.56. Thus, although there is a strong correlation between age and LTP at LOT synapses, there is no significant correlation at ASSN synapses.

Structural changes of neuronal morphology are correlated with critical periods for plasticity (Hensch, 2004), and increases in dendritic spine density during early development are associated with maturation of cortical circuits (Whitford et al., 2002). We next took advantage of the anatomical segregation of LOT and ASSN inputs to explore the early development of dendritic spines in these two pathways.

Pyramidal cells were filled with Alexa 488 (50 μM) and visualized using two-photon microscopy (Fig. 3A_1). We first examined dendritic spines ($n = 4720$) at distal apical and basal dendrites of pyramidal cells ($n = 84$) over the first postnatal month. Although ASSN inputs contact both proximal apical and basal dendrites, we initially focused on basal dendrites to control for branching order from the soma and to exclude possible contamination by the presence of sensory synapses. The distal apical dendrites we analyzed were at the broader of layer 1a and the LOT

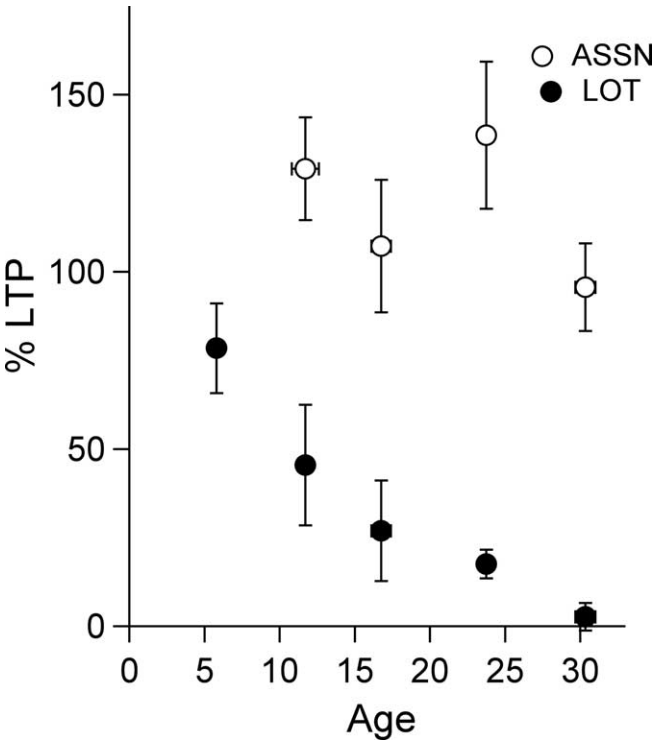

Figure 2. Summary data of the magnitude of LTP at LOT and ASSN synapses during the first postnatal month ($n = 3$–7 slices per point). The average LOT LTP magnitudes for age groups P5–P10, P11–P14, P15–P19, P20–P26, and P30–P35 were 78 ± 11, 45 ± 17, 26 ± 11, 17 ± 4, and 3 ± 3%, respectively. The average ASSN LTP magnitudes for age groups P11–P14, P15–P19, P20–P26, and P30–P35 were 129 ± 14, 107 ± 18, 138 ± 20, and 95 ± 12%, respectively.

(Fig. 3A_1). Spine lengths in both dendritic compartments were identical at age P5–P7 (apical: 2.61 ± 0.33 μm, $n = 7$ cells; basal: 1.85 ± 0.20 μm, $n = 4$ cells; $p = 0.08$) and became shorter with development (P34–P35; apical: 1.49 ± 0.04, $n = 10$ cells; basal: 1.34 ± 0.09, $n = 7$).

We next considered the developmental profile of spine density in dendritic compartments devoted to LOT and ASSN synapses. To rule out the possibility that intrinsic differences between apical and basal dendrites could govern the development of spine density, we imaged proximal apical dendrites in addition to distal apical and basal dendrites in a subsequent series of experiments ($n = 8721$ spines from 48 cells). Consistent with observations in other cortical areas (Whitford et al., 2002), we observed a significant increase in spine density of apical and basal dendritic compartments during development (Fig. 3A_2). However, the pooled data from all cells (Fig. 3*B*) indicated that spine density reached mature levels earlier at the site of LOT input (distal apical dendrites; exponential time constant of 3 d) versus compartments devoted to ASSN input (basal and proximal apical dendrites; exponential time constants of 12 and 16 d, respectively). Thus, as for synaptic plasticity, there is a brief developmental time window during which dendritic regions primarily devoted to sensory input undergo structural modification.

Discussion

In this study, we examined NMDAR-dependent plasticity and the structural maturation of sensory synapses in primary olfactory cortex. Our results indicate that during early development, sensory and ASSN synapses onto the same olfactory cortical pyramidal cells differ in their capacity for plasticity and spinogenesis.

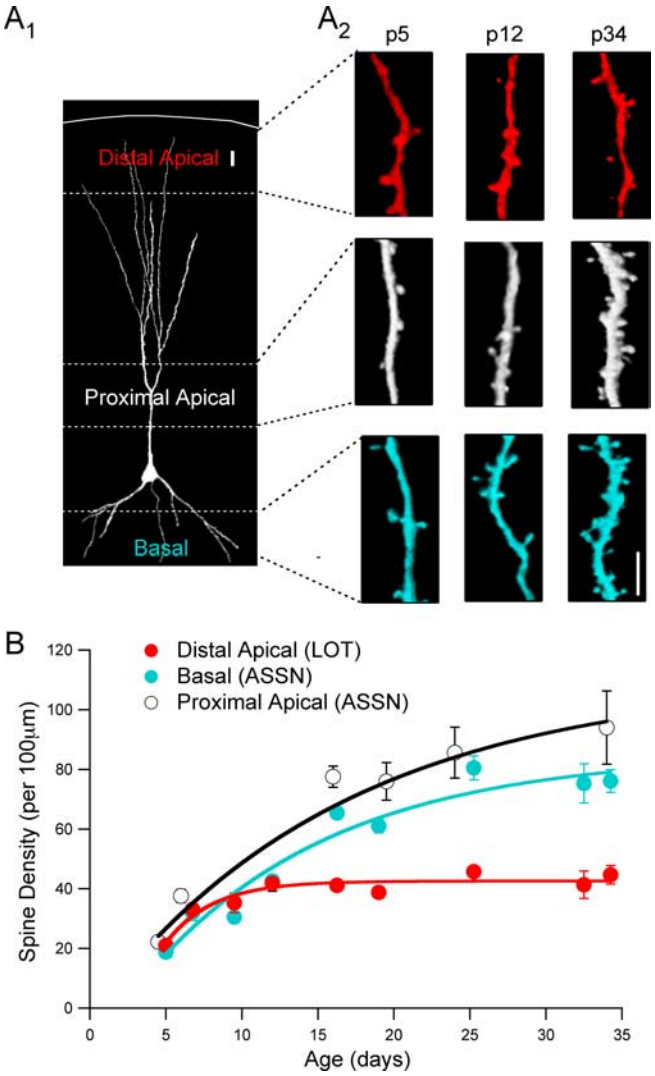

Figure 3. Developmental maturation of spine density occurs rapidly at dendrites receiving LOT input. ***A*$_1$**, Two-photon image of a representative pyramidal cell (P34). Dashed lines indicate boundaries from which distal apical, proximal apical, and basal dendritic spines were measured. The solid line represents pial surface. Scale bar, 20 μm. ***A*$_2$**, Distal apical (red), proximal apical (white), and basal dendritic (blue) regions from three cells at age P5, P12, and P34. Scale bar, 5 μm. ***B***, Developmental time course for increases in spine density at distal apical, proximal apical, and basal dendritic compartments. Each symbol represents values averages pooled over 2 d intervals. Distal apical spine density data for the nine age groups starting from P5–P6 to P34–P35 are as follows: 21 ± 0.9, 33 ± 1.5, 35 ± 3.3, 42 ± 1.6, 41 ± 0.8, 38 ± 1.0, 46 ± 1.5, 41 ± 4.6, and 45 ± 3.1 spines/100 μm; $n = \sim$12 cells for each age. Basal spine density data for the nine age groups starting from P5–P6 to P34–P35 are as follows: 19 ± 1.3, 32 ± 2.7, 31 ± 1.7, 43 ± 1.7, 65 ± 1.8, 61 ± 2.3, 80 ± 4.0, 75 ± 6.6, and 76 ± 3.8 spines/100 μm; $n = \sim$12 cells for each age. Proximal apical spine density data for the seven age groups starting from P5–P6 to P34–P35 are as follows: 22 ± 1.9, 38 ± 2.2, 41 ± 2.7, 77 ± 3.5, 76 ± 6.3, 86 ± 8.6, and 94 ± 12.3 spines/100 μm; $n = \sim$5 cells for each time point. Lines are exponential fits with time constants of 3, 12, and 16 d for distal apical, basal, and proximal apical dendrites, respectively.

Previous studies have established that NMDAR-dependent LTP is an important property of ASSN synapses in piriform cortex (Kanter and Haberly, 1990, 1993). Indeed, it has been suggested that activity-dependent plasticity of ASSN inputs could enhance the salience of odor-evoked responses in pyramidal cells and contribute to olfactory learning in adults (Quinlan et al., 2004; Lebel et al., 2006). However, a role for activity-dependent plasticity at the sensory afferent LOT synapses of olfactory cortex pyramidal cells is less clear. Although it has often been suggested

that LOT synapses can express NMDAR-dependent plasticity, several studies in adult rats using a range of tetanic stimulus protocols have shown only a modest and somewhat unreliable potentiation of LOT-evoked fEPSPs after tetanic stimulation (Jung et al., 1990; Kanter and Haberly, 1990; Stripling et al., 1991).

Our results using intracellular recording and pairing of stimulation with depolarization indicate that strong NMDAR-dependent LTP of LOT synapses occurs during a brief postnatal period, after which there is a decrease in the ability of LOT synapses to undergo potentiation with our pairing protocol. The gradual decline in pairing-induced LTP at LOT inputs is consistent with previous results indicating a marked developmental downregulation of NMDARs at sensory but not ASSN inputs (Franks and Isaacson, 2005). We believe that the rapid developmental loss of NMDARs at LOT synapses can explain why previous fEPSP studies in adult animals reported relatively unreliable and modest LTP. In contrast, the large, developmentally stable NMDAR component of synaptic transmission at ASSN synapses (Franks and Isaacson, 2005) would permit expression of synaptic plasticity in this pathway throughout adulthood.

We also observe marked differences in the structural maturation of dendritic compartments primarily devoted to LOT (distal apical dendrites) and ASSN (basal and proximal apical dendrites) input. Although we cannot rule out that some of the distal apical dendritic branches may receive ASSN inputs, these most distal branches undoubtedly receive predominantly LOT inputs. Basal dendrites, on the other hand, are solely targeted by ASSN. Although spine density increased during the first few postnatal weeks in both compartments, distal apical dendrites reached a plateau in spine density much earlier than basal dendritic regions. Proximal apical dendrites, which also receive ASSN input, showed a slow time course for spine density development that was quite similar to basal dendrites. Indeed, the maturation of LOT spine density is nearly complete by P9. This rate of maturation appears to be more rapid than other regions of sensory cortex where spine density increases dramatically beyond P9 (Miller and Peters, 1981; Micheva and Beaulieu, 1996). It may be that this early maturation of sensory dendritic regions in piriform cortex is associated with olfaction being completely functional in rodents at birth.

It is possible that the experience-dependent downregulation of NMDARs at sensory LOT synapses (Franks and Isaacson, 2005) could underlie both the critical period for LTP as well as the early maturation of dendritic spine density. For example, in addition to mediating activity-dependent plasticity, NMDARs are also thought to play a role in the development of dendritic spines (Lin et al., 2004; Tolias et al., 2005; Tada and Sheng, 2006). Studies have also shown *de novo* dendritic spinogenesis associated with NMDAR-dependent synaptic plasticity (Engert and Bonhoeffer, 1999; Maletic-Savatic et al., 1999). Thus, although the developmental time courses over which LTP at LOT inputs declines and spine density matures do not overlap completely, the similarities in their time courses suggest the possibility of a common underlying mechanism. Furthermore, even assuming a common underlying mechanism, divergent mechanisms for LTP expression and spinogenesis would most likely produce differences in the developmental profile of the two phenomena. An alternative possibility that we cannot exclude is that these observations arise from entirely independent mechanisms.

Together, the physiological and anatomical features of developing LOT synapses provide strong support for the notion that there is a critical period for the modification of olfactory input to the cortex. Our results are consistent with reports of critical periods for anatomical and synaptic plasticity in the visual (Wiesel and Hubel, 1963), somatosensory (Woolsey and Wann, 1976), and auditory (Zhang et al., 2001) cortices. The plasticity of developing olfactory sensory inputs could provide a substrate for enhancing the cortical representation of odors experienced during an early postnatal time window. The loss of activity-dependent LTP and the rapid maturation of the dendritic compartment targeted by LOT inputs suggest that there is a "hardwiring" of sensory synapses early in life. In contrast, the persistence of plasticity at ASSN synapses provides a basis for modifying the salience of odor information represented by pyramidal cells throughout adulthood.

References

Engert F, Bonhoeffer T (1999) Dendritic spine changes associated with hippocampal long-term synaptic plasticity. Nature 399:66–70.

Franks KM, Isaacson JS (2005) Synapse-specific downregulation of NMDA receptors by early experience: a critical period for plasticity of sensory input to olfactory cortex. Neuron 47:101–114.

Haberly LB (1998) Olfactory cortex. In: The synaptic organization of the brain, Ed 4 (Shepherd GM, ed), pp 377–416. New York: Oxford UP.

Haberly LB, Presto S (1986) Ultrastructural analysis of synaptic relationships of intracellularly stained pyramidal cell axons in piriform cortex. J Comp Neurol 248:464–474.

Hensch TK (2004) Critical period regulation. Annu Rev Neurosci 27:549–579.

Jung MW, Larson J, Lynch G (1990) Long-term potentiation of monosynaptic EPSPs in rat piriform cortex in vitro. Synapse 6:279–283.

Kanter ED, Haberly LB (1990) NMDA-dependent induction of long-term potentiation in afferent and association fiber systems of piriform cortex in vitro. Brain Res 525:175–179.

Kanter ED, Haberly LB (1993) Associative long-term potentiation in piriform cortex slices requires $GABA_A$ blockade. J Neurosci 13:2477–2482.

Katz LC, Shatz CJ (1996) Synaptic activity and the construction of cortical circuits. Science 274:1133–1138.

Lebel D, Sidhu N, Barkai E, Quinlan EM (2006) Learning in the absence of experience-dependent regulation of NMDAR composition. Learn Mem 13:566–570.

Leon M (1992) Neuroethology of olfactory preference development. J Neurobiol 23:1557–1573.

Lin H, Huganir R, Liao D (2004) Temporal dynamics of NMDA receptor-induced changes in spine morphology and AMPA receptor recruitment to spines. Biochem Biophys Res Commun 316:501–511.

Maletic-Savatic M, Malinow R, Svoboda K (1999) Rapid dendritic morphogenesis in CA1 hippocampal dendrites induced by synaptic activity. Science 283:1923–1927.

Micheva KD, Beaulieu C (1996) Quantitative aspects of synaptogenesis in the rat barrel field cortex with special reference to GABA circuitry. J Comp Neurol 373:340–354.

Miller M, Peters A (1981) Maturation of rat visual cortex. II. A combined Golgi-electron microscope study of pyramidal neurons. J Comp Neurol 203:555–573.

Mombaerts P (2001) How smell develops. Nat Neurosci [Suppl] 4: 1192–1198.

Nicoll RA, Malenka RC (1999) Expression mechanisms underlying NMDA receptor-dependent long-term potentiation. Ann NY Acad Sci 868:515–525.

Price JL (1973) An autoradiographic study of complementary laminar patterns of termination of afferent fibers to the olfactory cortex. J Comp Neurol 150:87–108.

Quinlan EM, Lebel D, Brosh I, Barkai E (2004) A molecular mechanism for stabilization of learning-induced synaptic modifications. Neuron 41:185–192.

Ressler KJ, Sullivan SL, Buck LB (1994) A molecular dissection of spatial patterning in the olfactory system. Curr Opin Neurobiol 4:588–596.

Stripling JS, Patneau DK, Gramlich CA (1991) Characterization and anatomical distribution of selective long-term potentiation in the olfactory forebrain. Brain Res 542:107–122.

Sullivan RM (2003) Developing a sense of safety: the neurobiology of neonatal attachment. Ann NY Acad Sci 1008:122–131.

Tada T, Sheng M (2006) Molecular mechanisms of dendritic spine morphogenesis. Curr Opin Neurobiol 16:95–101.

Tolias KF, Bikoff JB, Burette A, Paradis S, Harrar D, Tavazoie S, Weinberg RJ, Greenberg ME (2005) The Rac1-GEF Tiam1 couples the NMDA receptor to the activity-dependent development of dendritic arbors and spines. Neuron 45:525–538.

ul Quraish A, Yang J, Murakami K, Oda S, Takayanagi M, Kimura A, Kakuta S, Kishi K (2004) Quantitative analysis of axon collaterals of single superficial pyramidal cells in layer IIb of the piriform cortex of the guinea pig. Brain Res 1026:84–94.

Whitford KL, Dijkhuizen P, Polleux F, Ghosh A (2002) Molecular control of cortical dendrite development. Annu Rev Neurosci 25:127–149.

Wiesel TN, Hubel DH (1963) Effects of visual deprivation on morphology and physiology of cells in the cats lateral geniculate body. J Neurophysiol 26:978–993.

Woolsey TA, Wann JR (1976) Areal changes in mouse cortical barrels following vibrissal damage at different postnatal ages. J Comp Neurol 170:53–66.

Zhang LI, Bao S, Merzenich MM (2001) Persistent and specific influences of early acoustic environments on primary auditory cortex. Nat Neurosci 4:1123–1130.